European Conference on Optical Communication (ECOC) 2022 © Optica Publishing Group 2022

A Polarization-Independent Zig-Zag-Tilted Ovals Grating Coupler in a 0.25 µm Photonic BiCMOS Technology

Galina Georgieva[(1)], Pascal M. Seiler[(1,2)], Christian Mai[(2)], Anna Peczek[(2)], Klaus Petermann[(1)], Lars Zimmermann[(1,2)]

[(1)] Technische Universität Berlin, Departments of Hochfrequenztechnik-Photonik and Siliziumphotonik, Office HFT4, Einsteinufer 25, 10587 Berlin, Germany. galina.georgieva@tu-berlin.de
[(2)] IHP - Leibnitz Institut für innovative Mikroelektronik, Im Technologiepark 25, 15236, Frankfurt (Oder), Germany.

Abstract *A polarization-independent grating coupler, optimized for a low in-plane scattering and PDL is presented. It comprises an array of ovals with zig-zag orientations and is compatible with a 0.25 µm photonic BiCMOS technology. The wafer-averaged maximal PDL within a 20 nm bandwidth is 0.5 dB. ©2022 The Author(s)*

Introduction

There is a continuing competition between intensity modulated direct detection (IM-DD) and coherent detection as candidates to deliver the best solution for next generation data center interconnects (DCI)[1]. It is predicted that IM-DD will predominate in the next few years, but many attempts to make coherent detection competitive are ongoing. The focus is put on two crucial factors: 1) the minimization of the power consumption and 2) the reduction of the transceiver cost. With regard to the second factor, silicon (Si) photonic solutions are in the ascendant, exploiting the possibility to realize electronic-photonic intergrated circuits (EPIC), using standard (Bi)CMOS foundry processes[2]–[4]. For cost-effective, high-volume manufacturing platforms, wafer-level testing during technological development, during production, and during subsystem assembly, is of high importance[5]. Another decisive economic factor is the packaging cost. Therefore, grating couplers (GCs) are an established solution for optical interfacing, offering both wafer-scale testing capability and relaxed packaging tolerances. To enable dual-polarization (DP) coherent formats, polarization-splitting/combining 2D GCs are required. In this application field, the previous knowledge about 2D GCs needs to be revisited, especially with regard to the polarization handling. In the past, we analyzed several aspects that may prohibit the 2D GC's adoption in the target context. We have found that the limited polarization splitting in 2D GCs is an issue, leading to optical signal-to-noise-ratio (OSNR) penalties and coupling efficiency limitations[6],[7]. Moreover, the finite polarization split ratio is related to polarizations' non-orthogonality with a strong wavelength dependence[7]. In this paper, we show that a deteriorated polarization splitting is directly related to a large polarization dependent loss (PDL) at the receiver. Furthermore, we present a design approach, which is based on previously acquired knowledge about the physical origins of the polarization-related issues[8]. With our technique, a simultaneous optimization of the polarization split ratio, the polarizations' orthogonality and the PDL is possible. Compared to the well-known PDL-optimized 2D GCs by Luxtera[2], comprising a special scatterers' shape (see also Refs.[9]–[11]), the present design is distinguishable by its simplicity, making it suitable for a fabrication with a 248 nm deep UV lithography. Moreover, no optical proximity correction is necessary, further reducing fabrication costs. The proposed 2D GCs may also be adopted in wavelength-division multiplexed (WDM) systems.

Optimization Method and Simulation Results

In the following, the working principle of our 2D GCs will be explained. During the last years, we investigated extensively the 2D GC's cross-polarization, that is, the conversion of a given input polarization state to its orthogonal counterpart. For instance, if we have a y-polarized input field, the 2D GC converts it partially to a x-polarized field, assigned as a cross-polarization, see e.g. Fig. 1(a). In receiver-side 2D GCs, where polarization diversity is given, different combinations of a given target-polarization from one channel with the cross-polarization from the other channel will result. The most extreme cases are for the polarization states, depicted in Fig. 1(b). We assign them as an even- and

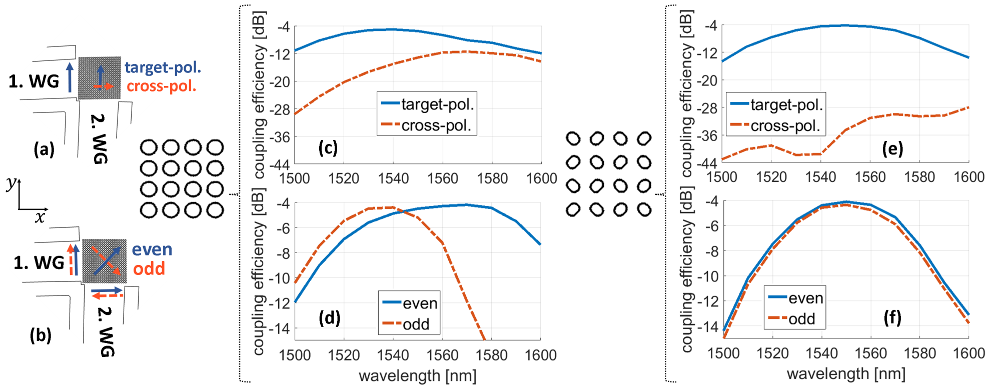

Fig. 1: A comparison between 2D GCs with circular and zig-zag-tilted oval perturbing elements. (a) A definition of a target- and cross-polarization, (b) a definition of an even- and odd-polarization. Coupling efficiency of a 2D GC with circular perturbing elements (c) target- vs. cross-polarization, (d) even- vs. odd-polarization. Coupling efficiency of a 2D GC with zig-zag-tilted oval perturbing elements (e) target- vs. cross-polarization, (f) even- vs. odd-polarization.

odd-polarization, depending on the symmetry of the split field components. An even-polarization is split to in-phase signals, e.g. a $+x$- and a $+y$-polarization. An odd-polarization is decomposed in anti-phase signals, e.g. a $-x$- and a $+y$-polarization. Accordingly, the superposition of a given target-polarization with the cross-polarization from the other channel will be in-phase or anti-phase. This results in a large PDL. Reference simulations are carried out for a 2D GC with circular perturbing elements. The 2D GC couples light to 2°-tilted 220 nm silicon-on-insulator rib waveguides with a rib etch depth equal to the grating etch depth (120 nm). The grating's perturbing elements have a 440 nm diameter and a periodicity of 622 nm for a C-band operation. The coupling angle at the symmetry plane is 8°. The target- and cross-polarization's coupling spectra can be seen in Fig. 1(c). The corresponding even- vs. odd-polarization relation is shown in Fig. 1(d) (y-component only, the x-component is the same, due to symmetry) . High levels of cross-polarization coupling can be observed in parallel with a large even-to-odd PDL.

The presence of a cross-polarization in receiver-side 2D GCs is a significant issue and its diminishment is decisive to reach low PDL. To reduce the cross-polarization strength, its physical background must be known. In a recent publication[8], we indicated in-plane scattering effects as the origin of cross-polarization in 2D GCs. Therefore, the reduction of the in-plane scattered fields is crucial. If we look at the reference 2D GC, we see that the perturbing elements are of identical size and shape so that each object has an identical scattering pattern. The periodic arrangement of the scattering objects with the same scattering profile leads to an enhanced cross-polarization. To avoid this, an abrupt change of the scattering

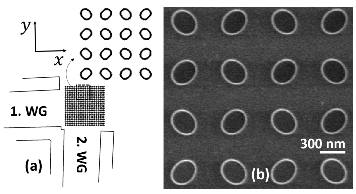

Fig. 2: An optimized 2D GC comprising a zig-zag-tilted ovals array: (a) a schematic representation, (b) an exemplary array after the reactive ion etch step.

pattern of adjacent objects can be advantageous. Here, we propose an optimization approach to reach that purpose, while keeping the perturbing elements' size, shape and periodicity constant. First, elongated objects such as ellipses or ovals may be chosen. Second, two adjacent elements may be rotated by $90°$ to each other. An exemplary design may result in a zig-zag-tilted ovals array as shown in Fig. 2. For an electromagnetic wave, propagating in x- or y-direction, a forwards-scattered field component will be superposed with a backwards-scattered one. Ideally, both components cancel each other. In reality, we pursue a sufficient suppression of the in-plane scattered fields and the corresponding cross-polarization, which can be achieved by the proper choice of the ovals' short and long diagonal. In the following example, it will be shown that this leads directly to a significant improvement of the PDL. A possible design comprises a waveguide-grating shear angle of 2°, a grating period of 594 nm, an etch depth of 140 nm, ovals with a short diagonal of 230 nm and a long diagonal of 320 nm. The feature sizes are well compatible with the 248 nm deep UV lithography, available in our fabrication platform[4]. The coupling angle remains 8°. Fig. 1(e) shows the simulated coupling efficiencies of the target- and cross-polarization of this structure. Fig. 1(f) shows the corresponding coupling spectra (y-component) of the even- and odd-polarization. A significant cross-polarization

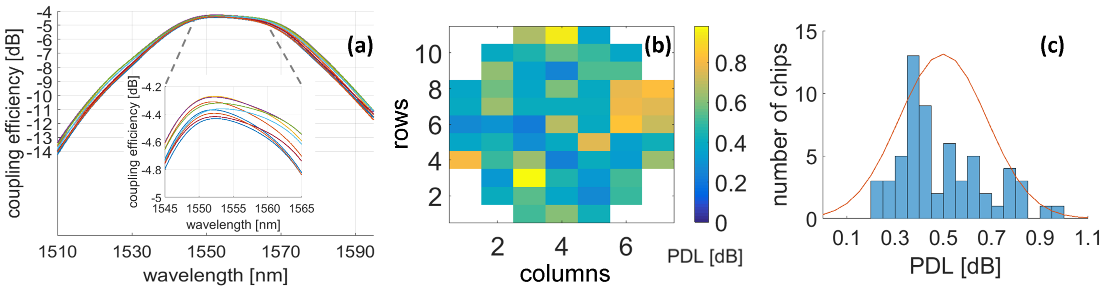

Fig. 3: Optimized 2D GC comprising a zig-zag-tilted ovals array. (a) Exemplary measured coupling spectra of different polarizations on a single chip. A zoom of the evaluation bandwidth from 1545 nm to 1565 nm is shown. (b) A wafer map and (c) a histogram of the maximal PDL within the considered bandwidth.

suppression is achieved, which results directly in a PDL below 0.5 dB in C-band. The coupling efficiency of all polarizations is centered at 1550 nm with a maximum of -4.1 dB. Another improved parameter is the transmitter-side orthogonality relationship between the polarizations, originating from both 2D GC arms[7]. In the reference model, the absolute deviation from the azimuth orthogonality state on the Poincaré sphere is $> 20°$ within C-band (similar to the structure in Ref.[7]). For the optimized model, this deviation is $< 3°$, ensuring almost uniform polarization angles within C-band.

Experimental Results and Conclusions

Back-to-back test structures, comprising two 2D GCs, connected by linear tapers and waveguides, are fabricated in a 0.25 µm photonic BiCMOS technology on 200 mm wafers with a partially processed backend of line stack. The stack height has no importance for the current investigation. The setup includes a tunable laser Agilent 81960A (1505 nm - 1625 nm), followed by a programmable polarization controller Agilent 8169A. Cleaved single-mode fibers (SMF) are used for in- and out-coupling. The signal is detected by a power meter Agilent 81634B. For the accurate power normalization, a slim photodiode S132Ce is placed in front of both SMF facets to measure the optical power loss in both off-chip paths, using a power meter PM100D by Thorlabs. Due to the short Si waveguides, no waveguide loss is considered. Full wafer measurements at a constant height are carried out on a semi-automated 300 mm wafer probe system by Formfactor. The fixed height does not correspond to the maximal power coupling. Different polarization states are scanned; for a fixed polarization state, a wavelength sweep is carried out. The first and the last measured spectra represent the same polarization state, and are used to control the coupling stability in the end of the polarization sweep. The PDL is determined in the following way. First, the wafer mean maximum transmission wavelength is found and 20 nm bandwidth around this wavelength is fixed. In this wavelength range, the maximal PDL is determined using 9 polarizations. The number of polarizations was found sufficient to find the maximal coupling efficiency difference within the given bandwidth. Finally, the PDL is averaged over the 61 chips on the wafer. Fig. 3(a) shows exemplary measured coupling spectra of different polarizations with a zoom in the considered bandwidth: the wafer-averaged central wavelength is 1555 nm with a mean coupling efficiency of -4.7 dB and a standard deviation σ of 0.2 dB. The 20 nm bandwidth considered for the PDL evaluation is from 1545 nm to 1565 nm. Fig. 3(b),(c) shows a wafer map and a histogram of the maximal PDL distribution. Because we could not use index-matching gel on this setup, there is an uncertainty in the PDL determination, caused by Fabry-Perot ripples. To reduce their impact, the measured curves are smoothed by a local regression fitting algorithm. The wafer maximal root-mean-square-error, representing the measurement uncertainty, is 0.1 dB. The wafer-averaged maximal PDL in the investigated wavelength range is 0.5 dB with σ of 0.18 dB. Furthermore, 67 % of the wafer chips have a maximal PDL $<$ 0.55 dB. Possibilities for further improvement of the fabrication process are currently under investigation.

In summary, we presented a simple design technique for 2D GCs for an improved polarization handling. Its feasibility was verified on wafer scale, achieving an averaged maximal PDL of 0.5 dB within a 20 nm bandwidth. In spite of the target application for DP coherent formats, the 2D GC's characteristics make it suitable for IM-DD systems as well. Future work will focus on solutions for O-band, which may be of interest not only for IM-DD, but also for coherent DCIs.[12].

We acknowledge partial support from the projects BMBF 13N14936, DFG ZI 1283-5-1, DFG ZI 1283-6-1 and DFG ZI 1283-7-1.

References

[1] X. Zhou, R. Urata, and H. Liu, "Beyond 1 Tb/s Intra-Data Center Interconnect Technology: IM-DD or Coherent?", *Journal of Lightwave Technology*, vol. 38, no. 2, pp. 475–484, 2020. DOI: 10.1364/JLT.38.000475.

[2] A. Mekis, S. Gloeckner, G. Masini, *et al.*, "A Grating-Coupler-Enabled CMOS Photonics Platform", *IEEE Journal of Selected Topics in Quantum Electronics*, vol. 17, no. 3, pp. 597–608, 2011. DOI: 10.1109/JSTQE.2010.2086049.

[3] M. Rakowski, C. Meagher, K. Nummy, *et al.*, "45 nm CMOS - Silicon Photonics Monolithic Technology (45CLO) for Next-Generation, Low Power and High Speed Optical Interconnects", in *Optical Fiber Communication Conference (OFC)*, San Diego, CA, USA, 2020, T3H.3. DOI: 10.1364/OFC.2020.T3H.3.

[4] D. Knoll, S. Lischke, A. Awny, *et al.*, "BiCMOS Silicon Photonics Platform for Fabrication of High-Bandwidth Electronic-Photonic Integrated Circuits", in *IEEE 16th Topical Meeting on Silicon Monolithic Integrated Circuits in RF Systems (SiRF)*, Austin, TX, USA, 2016, pp. 46–49. DOI: 10.1109/SIRF.2016.7445464.

[5] T. Pinguet, S. Denton, S. Gloeckner, *et al.*, "High-Volume Manufacturing Platform for Silicon Photonics", *Proceedings of the IEEE*, vol. 106, no. 12, pp. 2281–2290, 2018. DOI: 10.1109/JPROC.2018.2859198.

[6] G. Georgieva, K. Voigt, C. Mai, P. M. Seiler, K. Petermann, and L. Zimmermann, "Cross-Polarization Effects in Sheared 2D Grating Couplers in a Photonic BiCMOS Technology", *Japanese Journal of Applied Physics*, vol. 59, no. SO, SOOB03, 2020. DOI: 10.35848/1347-4065/ab8e21.

[7] G. Georgieva, P. M. Seiler, C. Mai, K. Petermann, and L. Zimmermann, "2D Grating Coupler Induced Polarization Crosstalk in Coherent Transceivers for Next Generation Data Center Interconnects", in *Optical Fiber Communications Conference and Exhibition (OFC)*, San Francisco, CA, USA, 2021, W1C.4. DOI: 10.1364/OFC.2021.W1C.4.

[8] G. Georgieva, K. Voigt, P. M. Seiler, C. Mai, K. Petermann, and L. Zimmermann, "A Physical Origin of Cross-Polarization and Higher-Order Modes in Two-Dimensional (2D) Grating Couplers and the Related Device Performance Limitations", *Journal of Physics: Photonics*, vol. 3, p. 035 002, 2021. DOI: 10.1088/2515-7647/abf942.

[9] J. Zou, Y. Yu, and X. Zhang, "Two-Dimensional Grating Coupler With a Low Polarization Dependent Loss of 0.25 dB Covering the C-band", *Optics Letters*, vol. 41, no. 18, pp. 4206–4209, 2016. DOI: 10.1364/OL.41.004206.

[10] Y. Sobu, S.-H. Jeong, and Y. Tanaka, "Si-wire Two-Dimensional Grating Coupler With Polarization-Dependent Loss of Lower Than 0.3 dB Over a 60-nm-wide Spectral Range", *Japanese Journal of Applied Physics*, vol. 57, p. 112 501, 2018. DOI: 10.7567/JJAP.57.112501.

[11] B. Chen, X. Zhang, J. Hu, *et al.*, " Two-Dimensional Grating Coupler on Silicon with a High Coupling Efficiency and a Low Polarization-Dependent Loss", *Optics Express*, vol. 28, no. 3, pp. 4001–4009, 2020. DOI: 10.1364/OE.380338.

[12] P. M. Seiler, G. Georgieva, G. Winzer, *et al.*, "Toward coherent O-band data center interconnects", *Frontiers of Optoelectronics*, vol. 14, no. 4, pp. 414–425, 2021. DOI: 10.1007/s12200-021-1242-0.